Bulletin of the Seismological Society of America, Vol. 96, No. 4A, pp. 1474–1482, August 2006, doi: 10.1785/0120050160

Site-Response Estimation for the 2003 Miyagi-Oki Earthquake Sequence Considering Nonlinear Site Response

by Kenichi Tsuda, Jamison Steidl, Ralph Archuleta, and Dominic Assimaki

Abstract The M_w 7.0 Miyagi-Oki earthquake, which occurred on 26 May 2003, was well recorded by the KiK-net and K-net networks. A large number of stations recorded very high peak ground accelerations above 0.5g and large peak ground velocities above 0.5 m/sec. These high ground-motion values are thought to come from a combination of the effect of shallow sediment layers of the upper couple of meters and the enhanced high-frequency ground-motion content associated with this intraslab earthquake. The objective of this study is to examine the effect of sediment amplification at network stations with peak ground acceleration $\geq$0.3g. Linear site response is first estimated from observed weak motion (aftershock) records. In this case, we use a spectral inversion method, without reference stations, to separate the source, path, and site-response effects. The resulting weak motion analysis for the source, path, and site response agree with other previous studies. The mainshock site response is obtained separately using the same spectral inversion technique with the addition of a frequency-dependent radiation pattern. The comparison of the site amplification from aftershocks with the mainshock indicates the possibility of nonlinear site response at many stations during the M_w 7.0 event. The results also suggest a correlation between low near-surface material velocity and the degree of nonlinearity.

Introduction

The 26 May 2003, M_w 7.0 Miyagi-Oki earthquake showed very large peak ground acceleration (PGA) at many stations (Satoh, 2004b). This event occurred within the subducting Pacific Plate (Yamanaka and Kikuchi, 2003). Although the hypocentral distance of most stations is greater than 80 km, there are many stations with large PGA, including some stations with PGAs greater than 1000 cm/sec^2 (gals). The horizontal PGA as a function of hypocentral distance at K-net (Kinoshita, 1998) and Kik-net (Aoi *et al.*, 2000) surface stations are shown in Figure 1. Also shown is the empirical attenuation curve proposed by Shi and Midorikawa (1999). This curve corresponds to the average relationship between PGA and hypocentral distance derived by using previously observed data. The observed PGA from this earthquake exceeded this empirical relationship, especially for stations at smaller distances. This earthquake generated large high-frequency ground motions, common to intraslab earthquakes (Morikawa and Sasatani, 2003) at close stations. Satoh (2004b) considered the effect of shallow sediment layers on top of the already high motions from the intraslab event as an additional reason for the observed large PGA. However, in that study, site response was relative to a reference site that had its own site response above 4 Hz. The site response of other stations was considered biased at frequencies above 4 Hz (Satoh, 2006).

The effect of local site conditions on earthquake ground motions have been documented as far back as the 1906 earthquake (Reid, 1910). Due in part to the inhomogeneous nature of the near-surface geology, every earthquake produces a spatial variation of ground motion and, consequently, spatial variability in the damage pattern. With the recent dense deployment of accelerometers in urban regions over the past 15 years, earthquakes such as the 1994 Northridge and 1995 Hyogo-ken Nanbu (Kobe) have clearly reinforced the role that site effects play in damaging ground motion (e.g., Kawase, 1996; Bonilla *et al.*, 1997; Hartzell *et al.*, 1997; Furumura and Koketsu, 1998). The data from the Miyagi-Oki earthquake provide a good opportunity to examine site response for a range of large accelerations that may be produced by the inevitable earthquakes that are certain to affect this highly active seismic region in the future, as well as many other active regions throughout the world.

To quantify site response, Borcherdt (1970) introduced the spectral ratio approach by taking ratios of the Fourier amplitude spectrum of soil sites to a rock site. This approach, and many variations of this that are reference site dependent, have been used to quantitatively examine site effects in the past. As mentioned already, previous studies of site response at the stations in this region were limited because of site effects at the "reference" site (Satoh, 2006). In this study, a

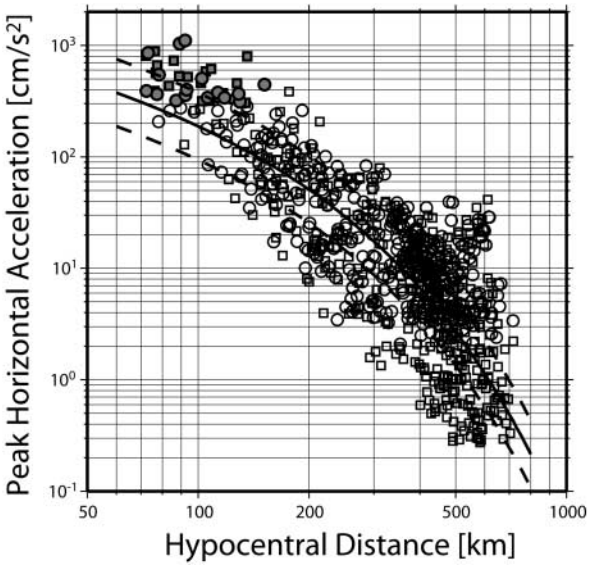

Figure 1. Peak horizontal accelerations as a function of hypocentral distance from 26 May 2003 Miyagi-Oki mainshock. The circles and squares correspond to the peak horizontal acceleration by K-net and KiK-net, respectively, with gray to denote the particular stations used in this study. A solid curve shows the empirical attenuation relationship calculated by Shi and Midorikawa (1999). The dashed lines correspond to the empirical relation ± a factor of 2.

method is used to estimate site response relative to seismological basement that does not rely on a particular station as the reference motion. Here we define the seismological basement as the depth where shear-wave velocities are ≥3.0 km/sec. Using borehole observations, we determine a reference source model for each event and an average reference path attenuation model that fits all the borehole data after a correction for potential borehole site response is made, Thus the site-response estimation technique in this study uses a theoretical source model and empirical seismological basement attenuation model as the reference.

Data

As previously noted, the *M* 7.0 Miyagi-Oki earthquake has many stations with PGA larger than 0.3*g* for the mainshock. We selected 16 K-net and 19 KiK-net stations with PGA ≥0.3*g*. In Figure 1, those stations are red to distinguish them from the many other observations of this earthquake. We also selected 14 aftershocks with $M_w > 4.0$. Hypocenter location and focal depths for these events are listed in the Table 1. We show the station distribution used in this study as well as the epicenter of mainshock and aftershocks in Figure 2. We use an *S*-wave time window of 10 sec for aftershocks and 20 sec for the mainshock starting approximately 1 sec before the *S*-wave arrival and apply a 5% cosine taper to the data window. The amplitude spectrum is then calculated by vector summation of the two horizontal components of the spectra. After we calculate the amplitude spectrum, we smooth the spectrum into 49 discrete points, *f*, from 0.5 to 20 Hz, by taking the average of the spectrum between $\pm f/10$ at each point.

Method

Observed ground motion can be expressed as a convolution of the source, path, and site. In the frequency domain, we can write this convolution as a multiplication:

$$|A(f)| = |S(f)||\mathrm{Site}(f)|R^{-1}\, e^{-\pi f R/Q(f)\beta} \qquad (1)$$

where f is frequency, $|A(f)|$ is the acceleration-amplitude spectrum of the recorded ground motion, $|S(f)|$ is the source spectrum, $Q(f)$ is the quality factor, which is assumed to be frequency dependent, $Q(f) = Q_0 f^{\gamma}$, $|\mathrm{Site}(f)|$ is the amplitude spectrum of the site response, R is the hypocentral distance, and β is the average shear-wave velocity between source and site (3.0 [km/sec]; Satoh *et al.*, 1997). In general, separating each element requires constraints to avoid trade-offs between the three elements. A standard constraint is to define $|\mathrm{Site}(f)|$ at a rock site (e.g., Bonilla *et al.*, 1997; Hartzell *et al.*, 1997; Satoh and Tastumi, 2002). Some KiK-net stations have the borehole sensor located in material very close to "seismological basement" (shear-wave velocity ≥3.0 km/sec). On the other hand, there are some stations with borehole sensors located in rock with shear-wave velocity about 0.6 km/sec. This indicates that the borehole records might also have a site response relative to "seismic basement." To remove the borehole response and to estimate absolute site response relative to the seismological basement, we applied the inversion scheme without using reference stations developed by Tsuda *et al.* (2005, 2006). This method is described subsequently in brief.

We assume Boatwright's (1978) representation of a ω^2 source spectrum (Brune, 1970) in equation (2). The amplitude of the source spectrum has a nonlinear dependence on the corner frequency:

$$|S(f)| = CM_0(2\pi f)^2 f_c^2/(f^4 + f_c^4)^{0.5} \qquad (2)$$

where

$$C = \frac{G_0 \cdot F^{\mathrm{rad}}}{4\pi\rho Vs^3} \qquad (3)$$

where C is depends on the radiation parameter of the source F^{rad} (we used 0.63 by Boore and Boatwright, 1984), the material parameters for source area (3.0 g/cc for density and 4.0 km/sec for shear-wave velocity; Satoh *et al.*, 1997), and the free surface effects, G_0. M_0 is the seismic moment that is related to the size of the earthquake and f_c is the corner frequency (Brune, 1970). The path effect also has a nonlinear dependence on frequency if we assume that the attenu-

ation parameter has a power law dependence on frequency $Q(f) = Q_0 f^{\gamma}$. Because of the nonlinear relationship between the data and some of the parameters, we use a Heat Bath algorithm (Sen and Stofa, 1995) to invert the four parameters: M_0, f_c, Q_0, and γ, and then with these source and path parameters, determine the frequency-dependent site response. In the aftershocks, we assume that the radiation pattern is stochastic ($C = 0.63$) because these events can be well represented by point sources.

We first determine path parameters Q_0 and γ and source parameters M_0 and f_c by using KiK-net borehole records of six aftershocks. These events have records at all of the 19 borehole stations. The detailed procedure is: (1) Solve for moment M_0 with the low-frequency data (0.5–1.0 Hz) using an initial model for the attenuation parameter, $Q(f) = 110 f^{0.67}$ (Satoh *et al.*, 1997). The effects of corner frequency can be considered negligible because of the size of the aftershocks (the corner is well above the frequency range used here). (2) Solve for the other three parameters: Q_0, γ, and f_c with M_0 fixed from the previous step for the entire frequency range (0.5–20 Hz). The difference between observed spectrum and synthetic spectrum based on those obtained parameters corresponds to the borehole response. (3) Repeat step 1 to determine the moment, but in this case, correcting the data for the borehole response and attenuation model obtained in the previous steps. The four parameters are solved by iteratively solving steps 2 and 3, until the residuals (borehole response) converge. (4) Last, we solve for M_0 and f_c again, this time for all 14 events separately by using the correction of borehole response and attenuation model determined in the previous steps.

Table 1
Event List Used in This Study

Date	M_w	Longitude	Latitude	Depth (km)
5/26, 18:24 (Main)	7	141.68	38.81	71
5/26, 22:34	4.6	141.6	38.89	76
5/27, 00:44	4.7	141.66	38.95	69
5/27, 10:47	4.5	141.68	38.75	66
5/27, 13:11	4.5	141.68	38.74	66
5/27, 21:12	4	141.64	38.96	68
5/28, 6:24	4.5	141.62	38.85	73
5/31, 1:33	4	141.62	38.78	68
5/31, 18:42	4.7	141.62	38.85	74
6/01, 5:38	4.2	141.61	38.86	74
6/10, 16:24	4.8	141.67	38.93	67
6/28, 20:19	4.3	141.58	38.81	72
7/14, 7:30	4.1	141.66	38.87	70
7/18, 12:32	4.4	141.59	38.28	75
7/21, 19:04	4.3	141.61	38.8	71

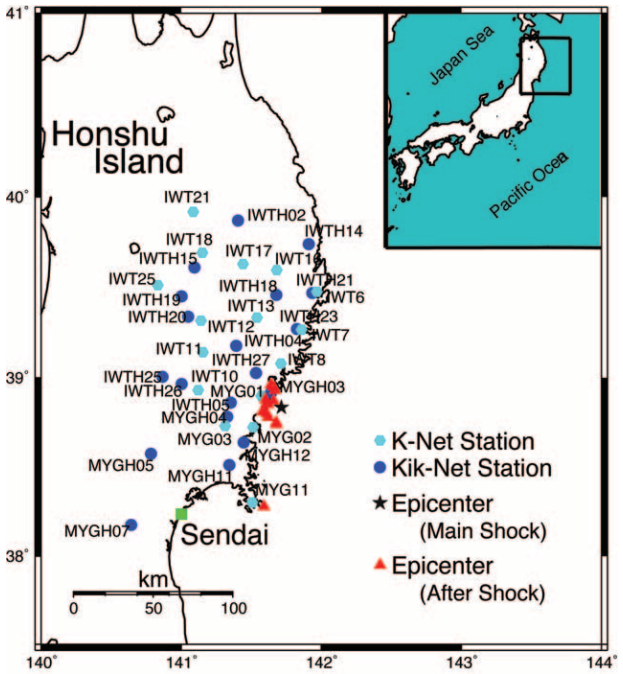

Figure 2. Station distribution of K-net (light-blue circle) and KiK-net (dark-blue circle) stations used in this study. The epicenter of mainshock (star) and 14 aftershocks (triangle) are also shown.

Now, having the source and path parameters for all of the events, we use equation (1) to predict the theoretical spectrum at all KiK-net surface stations and K-net stations for all aftershocks. This theoretical spectrum is considered the seismological basement motion at each site, or the "reference" motion. The difference between the predicted spectrum and the observed spectrum is the surface site response |Site(f)|. We average the results from the aftershocks to determine the final estimate of the site response at each surface station, and then compare with previous reference-site-based studies. Then we compare the aftershock site-response results with site response determined from the mainshock. The detailed procedure to estimate site response for "strong motion" (main shock) is explained in the following.

Site-Response Estimation from Mainshock

A basic assumption of the inversion applied to the aftershocks is the point-source approximation (i.e., not including finite-source effects implicitly). This assumption for the large earthquakes is sometimes not valid, however. Field *et al.* (1997, 1998) compared the site response from 1994 Northridge Earthquake mainshock and aftershocks and considered finite-source effects when they estimated site response from the mainshock. Given the wide azimuthal station distribution used in this study, we consider the effects of radiation pattern for the mainshock, because this is a large enough event that a point-source approximation no longer holds. When we determine the site response from the mainshock, we use the following assumptions. The borehole response for each KiK-net station and the attenuation model are common to those determined from the aftershocks (here we are assuming that nonlinear effects are not present at borehole depths). To consider the effects of focal mechanism, we incorporated a frequency-dependent radiation pat-

tern inside constant C in equation (3), assuming the function of frequency proposed by Kamae *et al.* (1990) as follows:

$$F^{\mathrm{rad}}(f) = \frac{(\log(f_2) - \log(f))F^0 + (\log(f) - \log(f_1))F^m}{\log(f_2) - \log(f_1)} \tag{4}$$

where F^0 is the theoretical radiation pattern coefficients (Aki and Richards, 2002) based on the geometry between hypocenter and station and focal mechanism (slip direction), and F^m is the averaged radiation pattern coefficient (0.63) for high-frequency range assuming isotropic radiation (Boore and Boatwright, 1984). Following the model proposed by Kamae *et al.* (1990), we use the theoretical radiation below f_1 Hz, isotropic radiation above f_2 Hz, and the radiation pattern for the range between f_1 and f_2 follow the shape of equation (4). In this study, we assume $f_1 = 0.5$ Hz and $f_2 = 5.0$ Hz. To calculate the theoretical radiation pattern, we used the moment-tensor focal-mechanism solution determined by broadband waveform inversion (strike, rake, dip = 190°, 69°, 97°; Fukuyama *et al.*, 1998). As for the initial values for estimating f_c, we use the following relationship between seismic moment and corner frequency obtained by Satoh *et al.* (1997).

$$\log M_0 = -3 \log f_c + 24.17 \tag{5}$$

The procedure to determine the M_0 and f_c is the same as the aftershocks, that is, try to fit the observed spectrum at the KiK-net borehole stations with the correction of borehole response and path effects.

Results

Source and Path Parameters

In Figure 3a, seismic moment obtained by our inversion results is compared with those obtained by NIED (National Research Institute for Earth and Disaster Prevention) (Fukuyama *et al.*, 1998). The two estimates of seismic-moment values are generally within a factor of 2 for the aftershocks as well as the mainshock. Seismic moment versus corner frequency is plotted in Figure 3b. Three lines corresponding Brune stress drops of 1 MPa, 10 MPa, and 100 MPa are also shown. Overall seismic moment scales with the inverse corner frequency cubed, indicating a constant stress drop of about 10 MPa. Although the stress drop from mainshock is relatively high (88 MPa) compared with subduction events, the high stress drop is similar to previous results for stress drop from intraplate events within the subducting plate (Morikawa and Sasatani, 2003; Satoh, 2004a). In addition, we show the flat level of acceleration source spectrum A, a function of the moment and corner frequency as calculated from (Dan *et al.*, 2001) and given in equation (3) next.

$$A = 4\pi^2 f_c^2 M_0 \tag{6}$$

This value usually correlates well with the energy radiated for the high-frequency range (Satoh, 2004a). In Figure 3c, we plotted the flat level A as a function of seismic moment. We also show the empirical relationship between them for the interplate subduction events proposed by Satoh and Tatsumi (2002). The flat level for the mainshock shows more than four times the previously determined empirical values. This indicates this mainshock radiated significantly more energy in the high-frequency range relative to interplate subduction events.

Attenuation results (quality factors) are shown in Figure 4. In this study, attenuation is assumed to be a function of frequency for whole frequency range studied. Also shown are attenuation models obtained in previous studies, including those specific to this area. Our attenuation model, $Q(f) = 92f^{0.88}$ agrees well with these other studies. The relatively large Qs value correlates with the trend pointed out by Satoh (2004b) that the attenuation is relatively small from intraslab earthquakes (Morikawa and Sasatani, 2003). The agreement of our source and path parameters with other independent studies indicates that the method is estimating the source and path effects properly.

Site Response

In Figure 5, we show the results of surface site response for K-net (Fig. 5a) and KiK-net (Fig. 5b) stations for weak (aftershock) motion. The site response (average $\pm$ 1σ) is plotted along with the site response from Satoh (2006) for comparison. Satoh (2006) applied the conventional inversion method with a reference-dependent constraint to estimate surface site response using weak motion data. In that analysis, one K-net station is used as the reference, so their site-response results are a relative value to that station. As pointed out in Satoh (2006), this "reference" station is amplified for frequencies higher than 4.0 Hz, so the site-response results are only valid up to 4 Hz. We compare our site-response results with those of Satoh (2006) in the valid range up to 4 Hz and find good correlation between the two methods in this frequency range. This comparison indicates our inversion scheme, without using a reference station, worked well to estimate surface site response for linear weak motions, at least for frequencies up to 4.0 Hz.

Next, we compare the site response determined from aftershocks with the mainshock site response estimates. In Figure 6, we plot the results of site response from the mainshock for K-net (Fig. 6a) and Kik-net (Fig. 6b) stations using a red line. We also plot site-response results from aftershock (average $\pm$ 1σ) using blue lines for comparison. The mainshock site responses from many stations show features often attributed to nonlinearity, such as a reduction of the site-response level in the high-frequency range and in some cases a shift of predominant frequency. Because many K-net stations are located on much softer sediments than those for KiK-net, the nonlinear phenomenon is expected to be more evident at K-net stations. Based on the velocity profiles dis-

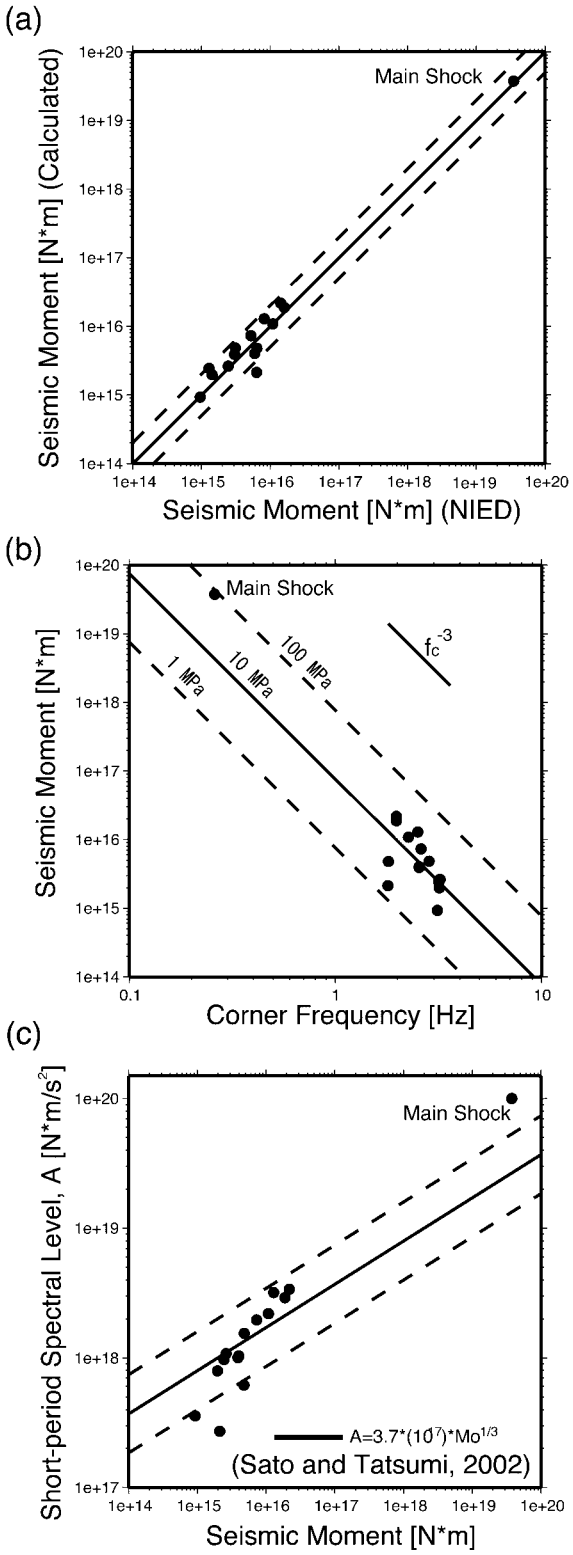

Figure 3. Obtained source parameters in this inversion analysis. (a) Seismic moments compared with that originally computed by NIED using a regional broadband network in Japan. (b) Seismic moment versus corner frequency with three lines corresponding the Brune stress drop, 1, 100 MPa (dash lines) and 10 MPa (solid line), respectively. (c) Relationship between flat level of acceleration source spectra A and seismic moment M_0. The solid line shows the empirical relationship derived by Satoh and Tatsumi (2002) for the interplate subduction events in Eastern Japan. The dashed lines correspond to a factor of 2 difference from the solid line.

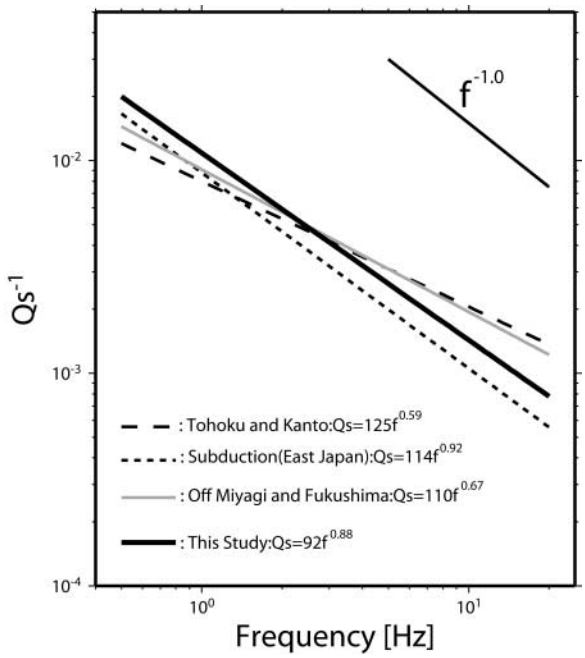

Figure 4. Comparison of Q^{-1} including our model of $Q(f) = 92f^{0.88}$ for the Off-Miyagi region. We also plotted other Q models obtained by data in Kanto and Tohoku area (Fukushima *et al.*, 1995), for subduction events in eastern Japan (Satoh and Tatsumi, 2002), and for the southern Tohoku area (Satoh *et al.*, 1997).

tributed by K-net (www.k-net.bosai.go.jp/k-net/), most stations used in this study have very soft sediment layers whose shear-wave velocities are smaller than 200 m/sec close to the surface. Stations such as IWT12 (V_s = 100 [m/sec]), MYG01 (V_s = 140 [m/sec]), MYG02 (V_s = 140 [m/sec]), MYG11 (V_s = 120 [m/sec]) all demonstrate clear nonlinear behavior in the mainshock site-response results. On the contrary, many Kik-net stations are usually located on hard sedimentary rock with thin soft sediment layers above them (www.kik.bosai.go.jp/kik/) like MYGH03 station. This station is located very close to the hypocenter (Fig. 2), but because its shear-wave velocity for the thin sediment layers are relatively large (350 [m/sec]), clear nonlinear phenomena are not seen even though the surface PGA level is quite high. The station MYGH07, located inside the Sendai Plain, shows a shift of predominant frequency and a reduction of site response for the mainshock. This could be attributed to nonlinear behavior of the very soft soil (V_s = 130 [m/sec]) in the upper 2 m. On average, the K-net stations (Fig. 6a) show more nonlinear features in the mainshock site-response results than the KiK-net stations (Fig. 6b).

Discussion and Conclusions

The spectral inversion method of Tsuda *et al.* (2005), using the "seismological basement" source spectrum and attenuation model determined from the KiK-net borehole ob-

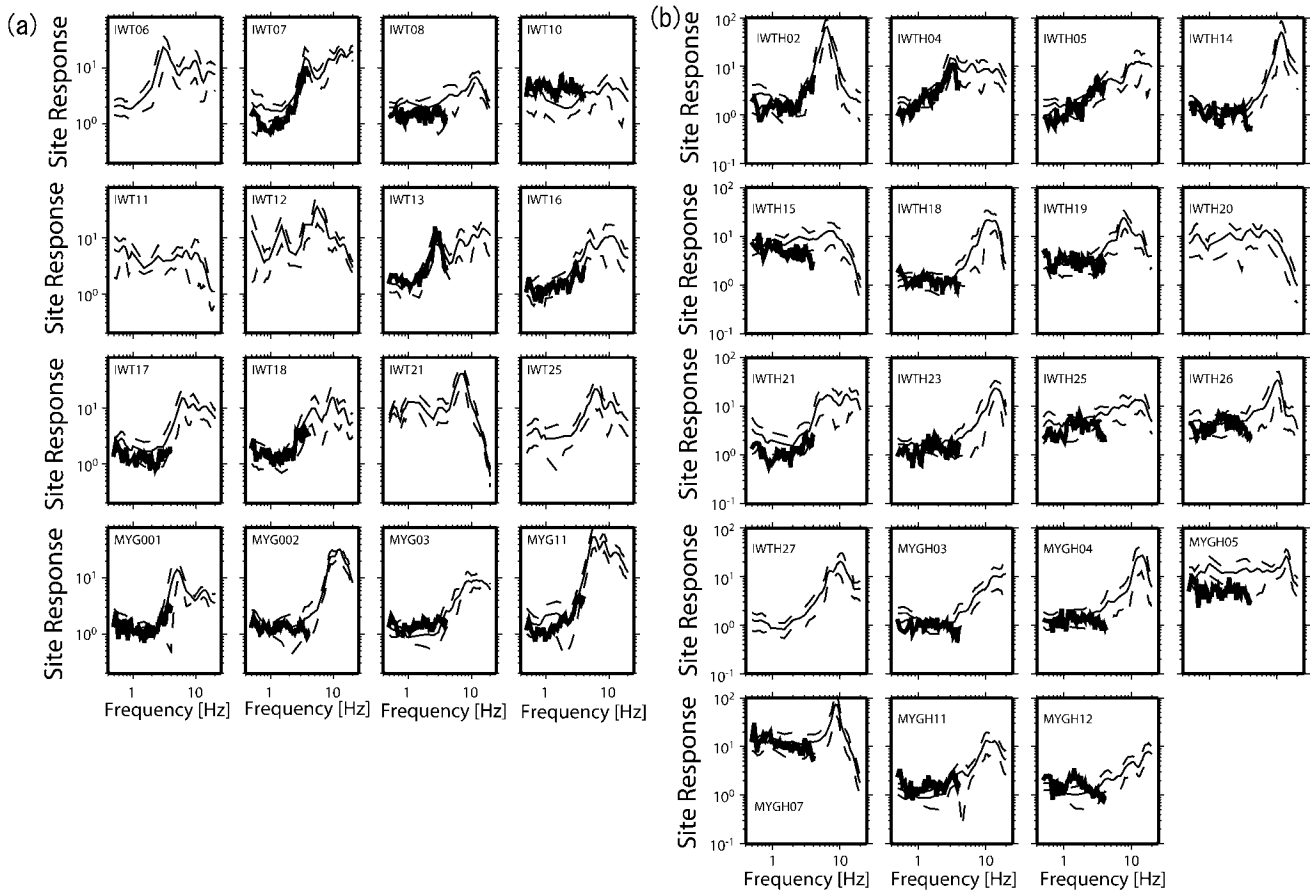

Figure 5. Surface site response derived by the observed data for K-net (a) and Kik-net (b) stations (light black lines with average $\pm$ 1σ). Site-response results from conventional inversion analysis by Satoh (2006) are also shown (bold black lines).

servations, is shown to provide good results on the estimation of site response in both the weak-motion case, and, with some modifications for finite-fault radiation, for the strong-motion case. The comparison of site response from the mainshock with the average aftershock site response suggests nonlinear site response during the mainshock was a factor for many stations with PGA $\geq$0.3g at the K-net and, to a lesser extent, the KiK-net networks. Asano *et al.* (2004) constructed a source model assuming linear site response (e.g., Aguirre *et al.*, 1994) and mentioned that the overestimation of predicted PGA from synthetic ground motions based on their source model indicates the possibility of nonlinear site response, supporting our results.

The degree of nonlinear soil behavior seems to correlate with the site conditions. Stations from the K-net network, which tend to have softer near-surface velocity structure, also tend to have larger reductions in site response when comparing the mainshock with the average aftershock site response. The stations from the KiK-net network also show what could be interpreted as evidence of nonlinear site response for the mainshock, but this effect is not as significant for the group of stations on average, as for the K-net stations. This can be explained by the stiffer material properties in the near-surface at the KiK-net stations.

Although most of the stations from K-net and KiK-net have subsurface information about velocity structure, the parameters that are used to define the soil behavior during earthquake loading at large strain, such as the maximum strength of the material, modulus degradation, and damping curves, are not readily available. Dynamic modeling of the strong-motion observations using the KiK-net borehole records as input motion will be the subject of a future study to evaluate the sensitivity of constitutive model parameters on the resulting fully nonlinear simulations based on the given constitutive relation (e.g., Bonilla *et al.*, 2005), and to compare with linear and equivalent linear simulations of the site response. Preliminary results at estimating the change in shear-wave velocity for strong-motion observations and comparison between linear, equivalent linear, and nonlinear methods for simulating dynamic soil behavior for the Miyagi-Oki mainshock can be found for a few of these stations in Assimaki and Steidl (2006) and Tsuda *et al.* (2005).

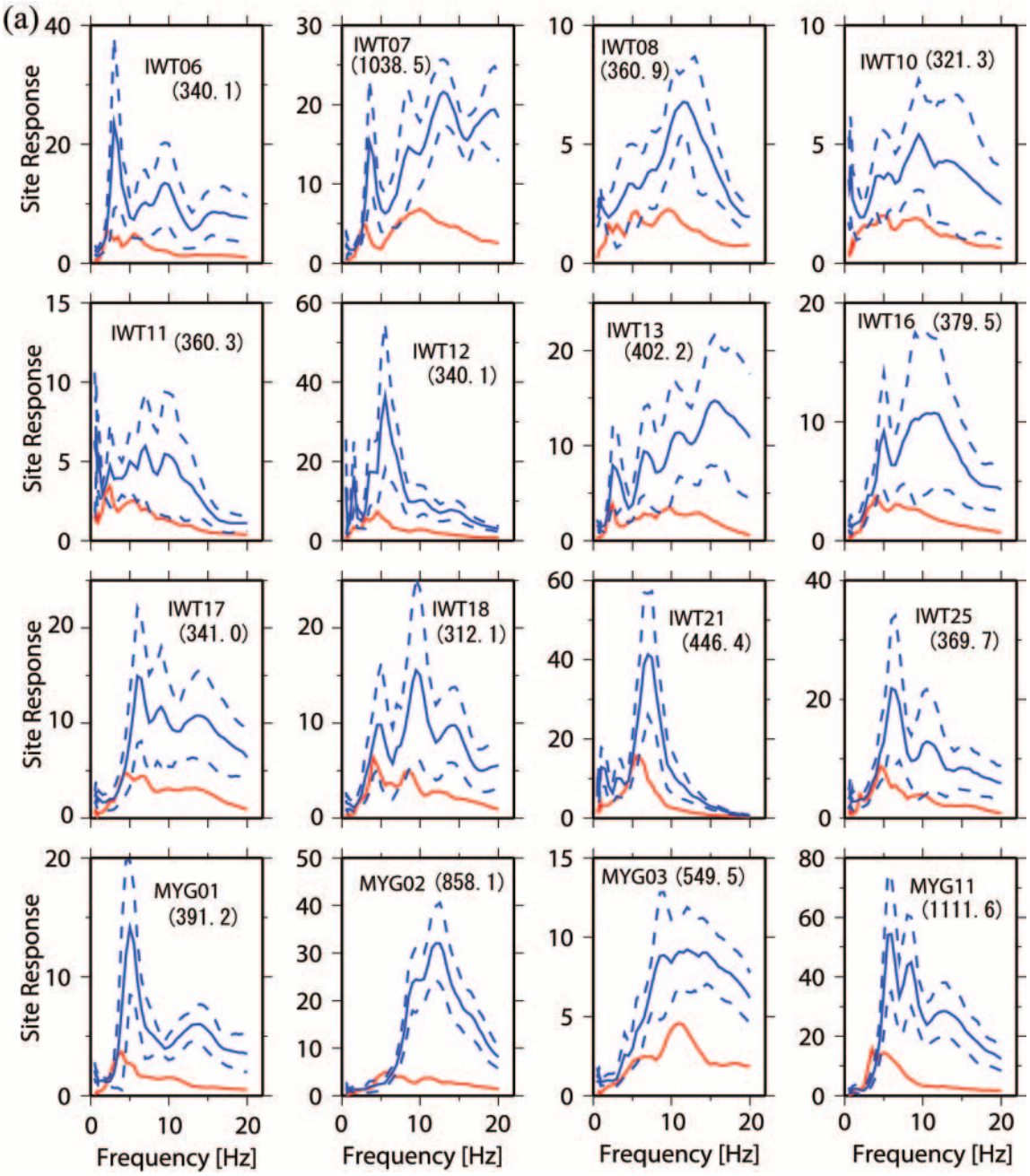

Figure 6. Surface site response derived from the observed data for K-net (a) and Kik-net (b) stations. The blue lines correspond to the average site response from weak-motion data (average $\pm$ 1σ) and the red line corresponds to the mainshock site response. The value in the parentheses is the maximum PGA recorded at the surface for each site in cm/sec^2. (*continued*)

Acknowledgments

This study would not be possible without the data from the well-managed KiK-net and K-net networks obtained through NIED. T. Satoh at Shimizu Corp. kindly provided her results for comparison. We thank H. Nakahara at Tohoku University for his careful reading and comments. Discussions about nonlinear site response with F. Bonilla were very helpful. The comments by A. Pitarka and an anonymous reviewer were very useful in improving this manuscript. We used the generic mapping tools by Wessel and Smith (1998) to produce most figures. This paper is ICS Contribution No. 0694.

References

Aguirre, J., K. Irikura, and K. Kudo (1994). Estimation of strong ground motion on hard rock and soft sediment sites in Ashigara valley using the empirical Green's function method, *Bull. Disast. Prev. Res. Inst., Kyoto Univ.* **44,** 45–68.

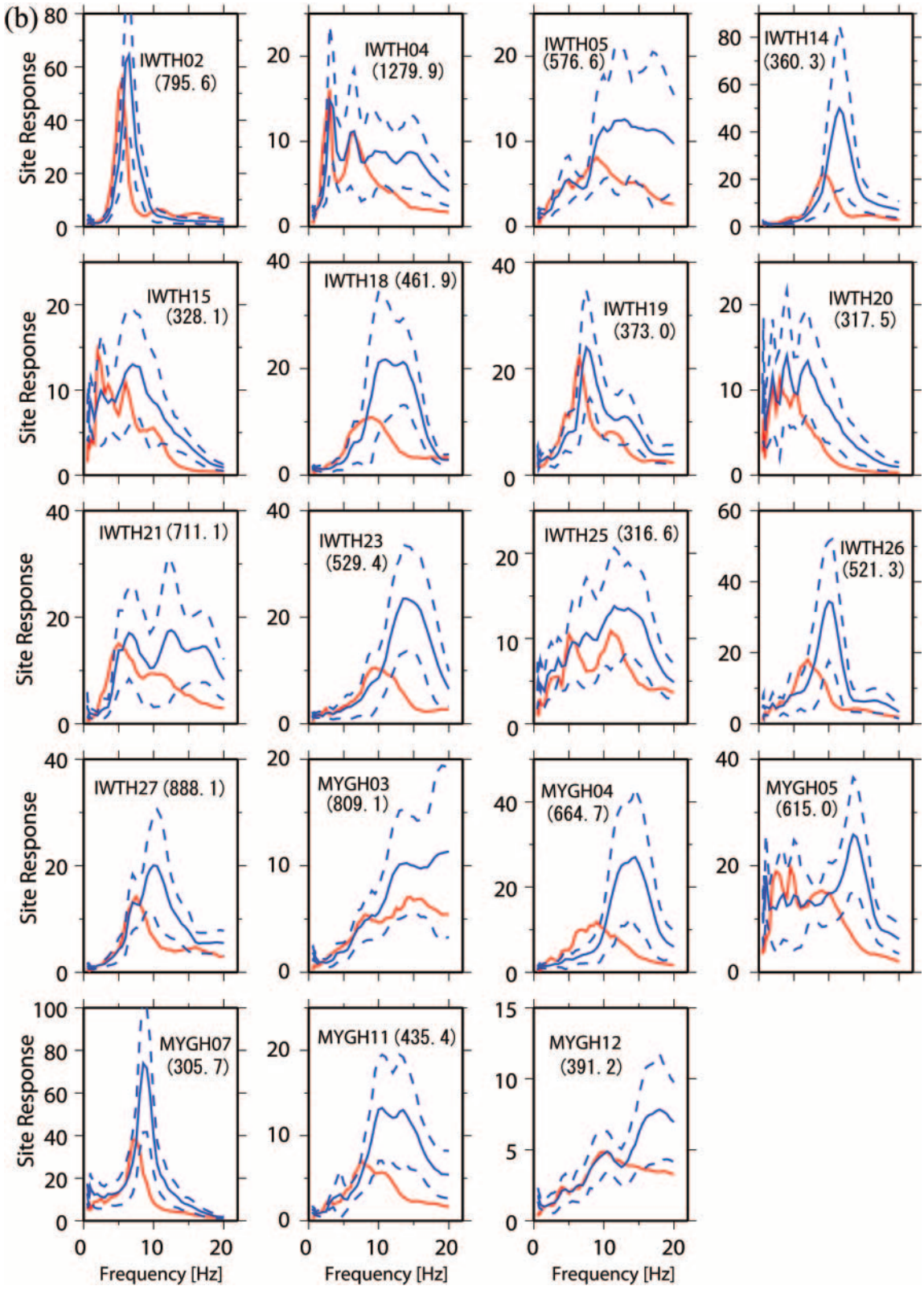

Figure 6. Continued.

Aki, K., and P. G. Richards (2002). *Quantitative Seismology*, Second Ed., University Science Books, Sausalito, CA.

Aoi, S., K. Obara, S. Hori, K. Kasahara, and Y. Okada (2000). New strong motion observation network KiK-net, *EOS Trans. AGU*, **81,** no. 48.

Asano, K., T. Iwata., and K. Irikura (2004). Source modeling and strong ground motion simulation of the off Miyagi interslab earthquake of May 26, 2003, *Zishin* **57,** 171–185 (Japanese with English abstract).

Assimaki, D., and J. Steidl (2006). Inverse analysis of weak and strong motion down hole array data from the M_w 7.0 Sanriku-Minami earthquake, *Soil Dyn. Earthquake Eng.* (in press).

Boatwright, J. (1978). Detailed spectral analysis of two small New York State earthquakes, *Bull. Seism. Soc. Am.* **68,** 1117–1131.

Bonilla, L. F., R. Archuleta, and D. Lavalèe (2005). Hysteretic and dilatant behavior of cohesionless soils and their effects on nonlinear site response: field data observations and modeling, *Bull. Seism. Soc. Am.* **95,** 2373–2395.

Bonilla, L. F., J. H. Steidl, G. T. Lindley, A. G. Tumarkin, and R. J. Archuleta (1997). Site amplification in the San Fernando valley, California: variability of site-effect estimation using the S-wave, coda, and H/V methods, *Bull. Seism. Soc. Am.* **87,** 710–730.

Boore, D. M., and J. Boatwright (1984). Average body-wave radiation coefficient, *Bull. Seism. Soc. Am.* **74,** 1615–1621.

Borcherdt, R. D. (1970). Effects of local geology on ground motion near San Francisco Bay, *Bull. Seism. Soc. Am.* **60,** 29–61.

Brune, J. N. (1970). Tectonic stress and the spectra of seismic shear waves from earthquakes, *J. Geophys. Res.* **75,** 4997–5009.

Dan, K., M. Watanabe, T. Sato, and T. Ishii (2001). Short-period source spectra inferred from variable-slip rupture models and modeling of earthquake fault for strong motion prediction, *J. Struct. Constr. Eng.* **545,** 51–62 (Japanese with English abstract).

Field, E. H., Y. Zeng, P. A. Johnson, and I. A. Beresnev (1998). Pervasive nonlinear sediment response during the 1994 Northridge earthquake: observations and finite-source simulations, *J. Geophys. Res.* **103,** 26,869–26,883.

Field, E. H., P. A. Johnson, I. A. Beresnev, and Y. Zeng (1997). Nonlinear ground-motion amplification by sediments during the 1994 Northridge earthquake, *Nature* **390,** 599–602.

Fukushima, Y., J.-C. Gariel, and T. Tanaka (1995). Site-dependent attenuation relations of seismic motion parameters at depth using borehole data, *Bull. Seism. Soc. Am.* **85,** 1790–1804.

Fukuyama, E., M. Ishida, D. S. Dreger, and H. Kawai (1998). Automated seismic moment tensor determination by using on-line broadband seismic waveforms, *Zishin* **51,** 149–156 (Japanese with English abstract).

Furumura, T., and K. Koketsu (1998). Specific distribution of ground motion during the 1995 Kobe earthquake and its generation mechanism, *Geophys. Res. Lett.* **25,** no. 6, 785–788.

Hartzell, S., E. Cranswick, A. Frankel, D. Carver, and M. Meremonte (1997). Variability of site response in the Los Angels urban area, *Bull. Seism. Soc. Am.* **8,** 1377–1400.

Kamae, K., K. Irikura, and Y. Fukuchi (1990). Prediction of strong ground motion for M7 earthquake using regional scaling relations of source parameters, *J. Struct. Constr. Eng.* **416,** 57–70 (Japanese with English abstract).

Kawase, H. (1996). The cause of the damage belt in Kobe: the basin edge effects, constructive interference of the direct S-wave with the basin-induced diffracted/Rayleigh waves, *Seism. Res. Lett.* **67,** 25–34.

Kinoshita, S. (1998). Kyoshin Net (K-Net), *Seism. Res. Lett.* **69,** 309–332.

Midorikawa, S. (1993). Nonlinearity of site amplification during strong ground shaking, *Zishin* **46,** 207–216 (Japanese with English abstract).

Morikawa, N., and T. Sasatani (2003). Source spectral characteristics of two large intra-slab earthquakes along the southern Kurile-Hokkaido arc, *Phys. Earth Planet. Interiors* **137,** 67–80.

Reid, H. F. (1910). The California earthquake of April 18, 1906, Publication 87, Vol. 21, Carnegie Institute of Washington, Washington, D.C.

Satoh, T. (2004a). Short-period spectral level of intraplate and interplate earthquakes occruring off Myagi prefecture, *J. JAEE* **4,** 1–4 (Japanese with English abstracts).

Satoh, T. (2004b). Study on causes of large peak accelerations of the 2003 Miyagiken-oki earthquake based on strong ground motion records, *J. Struct. Constr. Eng.* **581,** 31–38 (Japanese with English abstract).

Satoh, T. (2006). Influence of fault mechanism, depth, and region on stress drops of small and moderate earthquakes in Japan, *Struct. Eng./Earthquake Eng.* **27,** 125–134.

Satoh, T., and Y. Tatsumi (2002). Source, path, and site effects for crustal and subduction earthquakes inferred from strong motion records in Japan, *J. Struct. Constr. Eng.* **556,** 15–24 (Japanese with English abstract).

Satoh, T., M. Fushimi, and Y. Tatsumi (2001). Inversion of strain-dependent nonlinear characteristics of soils using weak and strong motions observed by borehole sites in Japan, *Bull. Seism. Soc. Am.* **91,** 365–380.

Satoh, T, H. Kawase, and T. Sato (1997). Statistical spectral model of earthquakes in the Eastern Tohoku district, Japan, based on the surface and borehole records observed in Sendai, *Bull. Seism. Soc. Am.* **87,** 446–462.

Sen, K. M., and P. L. Stoffa (1995). *Global Optimization Methods in Geophysical Inversion*, Elsevier, New York.

Shi, H., and S. Midorilkawa (1999). New attenuation relationships for peak ground acceleration and velocity considering effects of fault type and site condition, *J. Struct. Constr. Eng.* **523,** 63–70 (Japanese with English abstract).

Tsuda, K., R. Archuleta, and K. Koketsu (2006). Quantifying spatial distribution of site response by use of the Yokohama High-Density Strong Motion Network, *Bull. Seism. Soc. Am.* (in press).

Tsuda, K., R. Archuleta, and J. Steidl (2005). Nonlinear site response: case study from 2003 and 2005 Miyagi-Oki Earthquakes, in *International Workshop on Strong Ground Motion Prediction and Earthquake Tectonics in Urban Areas*, pp. 115–118.

Wessel, P., and W. H. F. Smith (1998). New improved version of the Generic Mapping Tools released, *EOS Trans. AGU* **79,** 579.

Yamanaka, Y., and M. Kikuchi (2003). May 26, Miyagi-oki earthquake (Mj = 7.0), *EIC Seism. Notes* **135,** www.eic.eri.u-tokyo.ac.jp/EIC/EIC News/030526n.html (last accessed May 2006).

Department of Earth Science and Institute for Crustal Studies
University of California
Santa Barbara, California 93106-1100
(K.T., R.J.A.)

Institute for Crustal Studies
University of California
Santa Barbara, California 93106-1100
(J.S.)

Civil and Environmental Engineering Department
Georgia Institute of Technology
Atlanta, Georgia 30332
(D.A.)

Manuscript received 28 July 2005.